Pergamon

Int. J. Solids Structures Vol. 35, Nos 34-35, pp. 4659–4683, 1998

Printed in Great Britain
0020–7683/98/$—see front matter

PII: S0020–7683(98)00089–4

A COUPLED THERMOPOROELASTIC MODEL WITH THERMO-OSMOSIS AND THERMAL-FILTRATION

Y. ZHOU, R. K. N. D. RAJAPAKSE† and J. GRAHAM
Department of Civil and Geological Engineering, University of Manitoba, Winnipeg, Canada R3T 5V6

(*Received* 26 *October* 1996; *in revised form* 17 *February* 1998)

Abstract—A coupled thermoporoelastic model accounting for compressibility and thermal expansion of constituents, convective heat flow and changing porosity and related properties of a saturated soil is presented. The model also considers thermodynamically coupled water and heat flow (thermal-filtration and thermo-osmosis that are analogous to Sorêt and Dufour effects in solutions). These coupling effects are reported to be significant in the case of semi-impermeable clay barriers used in waste repositories. The governing equations derived in terms of displacements, temperature and pore water pressure are non-linear. A mixed finite element formulation is presented to obtain numerical solutions. An exact analytical solution for a 1-D soil column is presented for a simplified linear case that includes thermodynamic coupling. Selected numerical solutions for soil columns and radially symmetric plane strain problems are presented to demonstrate the principle features of the coupled model and the significance of thermodynamic coupling. © 1998 Elsevier Science Ltd. All rights reserved.

INTRODUCTION

Coupled heat-fluid flow in a saturated deformable porous medium is important in many branches of engineering. Applications can be found in diverse areas such as geothermal energy extraction, petroleum engineering, chemical engineering, agricultural engineering, geotechnical engineering, pavement engineering, hazardous waste management and biomechanics. In recent years, this topic has generated considerable attention in the field of nuclear waste management. For example, the Canadian program for management of nuclear wastes proposes to store titanium canisters containing spent fuel rods in a deep geologic vault to be built in the Canadian shield. A sand–bentonite mixture will be placed as a buffer between the canister and the surrounding rock. Complex thermoporoelastic fields can be expected in and around the waste repository due to temperature and fluid pressure gradients created by emplacement of the canisters.

The sand–bentonite buffer that has been proposed for waste disposal will be initially unsaturated with a degree of saturation $S_r = 85\%$. Coupled heat-moisture flow in an unsaturated medium is a complicated problem that requires consideration of a multi-component system consisting of air, vapour, water and soil skeleton. As an initial step in solving this complicated system, the solution described in the following pages deals only with fully saturated soils ($S_r = 100\%$). However it takes account of fully coupled thermo-hydro-mechanical effects and material property changes that result from changes in stresses, hydraulic gradient, and temperature gradient.

The development of continuum theories for coupled processes of heat–fluid flow and deformation in saturated media has received considerable attention in the past. The seminal work of Biot (1941, 1956) described the consolidation of a soil under isothermal conditions. Rice and Cleary (1976) recast the Biot's formulation in terms of more easily identifiable material parameters such as the drained and undrained elastic moduli and Skempton's pore water pressure parameters. Detournay and Cheng (1993) and Senjuntichai (1994) reviewed Biot's poroelastic theory and its applications to a variety of quasi-static and dynamic

† Author to whom correspondence should be addressed. Tel.: 001 204 474 8068. Fax: 001 204 474 7513. E-mail: rajapak@cc.umanitoba.ca

problems. Biot (1956, 1977) also extended his isothermal theory to include thermal effects on consolidation. A rigorous mathematical treatment of the present class of problems can also be established within the framework of a general theory of mixtures (Adkins, 1963). Formulation of this type, taking into account various non-linear effects was used by Bowen (1982) to study deformable, non-isothermal media with multiple pore fluids. Adkin's formulation has rarely been used in engineering applications because it requires several constitutive functionals which are difficult to determine experimentally.

Following the basic framework of Biot (1956), several authors (for example, Schiffman, 1971; Derski and Kowalski, 1979; Bear and Corapcioglu, 1981; Palciauskas and Domenico, 1982; Booker and Savvidou, 1985; McTigue, 1986; Kurashige, 1989; Lewis and Schrefler, 1987; Smith and Booker, 1993; Jiang and Rajapakse, 1994; Seneviratne *et al.*, 1994) studied the non-isothermal behaviour of fluid-saturated media. These studies differ only in details. They are based on varying assumptions that may include incompressibility of constituents, small temperature variations, thermal equilibrium of solid and fluid phases, linear elastic behaviour of the solid phase, non-convective heat flow, absence of phase change of fluid, constant material properties, etc. Booker and Savvidou (1985), McTigue (1986, 1990), Smith and Booker (1993) and Jiang and Rajapakse (1994) presented analytical solutions for thermoporoelastic models with constant material properties subjected to small perturbations about an initial state. Finite element solutions for thermoporoelasticity were presented by Lewis and Schrefler (1987), Britto *et al.* (1992) and Seneviratne *et al.* (1994). All of the above solutions are based on conventional Darcy and Fourier laws for fluid flow and heat flow, respectively. They therefore neglect the influences of pressure gradient on heat flow (thermal-filtration which is analogous to Dufour effects in solutions) and the temperature gradient on fluid flow (thermo-osmosis effect which is analogous to Sorêt effect in solutions). Thermo-osmosis and thermal-filtration are coupled processes which arise as a consequence of thermodynamics of irreversible processes (Fitts, 1962; Onsager, 1931).

Experimental studies (McVay, 1984) indicate that large water pressure and temperature gradients can be generated in the near-field of a nuclear fuel-waste disposal facility after the emplacement of waste canisters. These gradients become the primary driving forces of complex thermoporoelastic fields. Carnahan (1984) showed that the near-field fluid flow in a semi-impermeable clay barrier due to thermodynamically coupled effects (thermo-osmosis) can be substantially higher than that due to the direct effect of Darcian flow. Thermodynamically coupled transport processes in soil-water systems have been studied in soil sciences and geohydrology for many years (Groenevelt and Bolt, 1969). However these studies exclusively neglect deformations and stresses of the soil.

In the confined conditions in a large repository, heating will cause increased pore water pressures (Hueckel and Pellegrini, 1992; Tanaka and Graham, 1996). These can produce decreased strength in buffer or in clay beds. The outcome could be decreased support for containers, or initiation of tensile cracking leading to hydraulic fracture.

Clay barriers proposed for waste disposal have very low hydraulic conductivity (10^{-10}–10^{-14} m/s). Under these conditions, thermo-osmosis becomes significant in the presence of expected temperature gradients. The effect can generally be neglected in traditional geotechnical engineering applications since the hydraulic conductivities are usually higher and the temperature gradient is often negligible. However for environmental protection and public safety reasons, it cannot be neglected in the planning and design of nuclear fuel waste disposal facilities. Experimental determination of the phenomenological coefficients associated with thermodynamically coupled transport processes are discussed by Letey and Kemper (1969) and Srivastava and Avasthi (1975). Existing studies on thermoporoelasticity neglect thermodynamically coupled heat and fluid flow. McTigue (1986) briefly mentioned coupled effects but did not include these effects in the analysis. Coussy (1995) recently discussed the effects of thermodynamically coupled flow within the framework of deformable porous media. Although Carnahan (1984) showed the significance of these effects on semi-impermeable clay barriers, he did not present a thermoporoelastic theory to account for coupled effects. No solution appears to be available that accounts for thermodynamically coupled heat and fluid flow, compressibility and thermal expansion of constituents, and changing material properties. This forms the basis of the present paper.

The model can be used for quantifying the significance of coupling between various driving forces and also in evaluating the applicability of semi-coupled models reported in the literature. It will also be useful in other applications such as energy resource explorations, pavement engineering, etc.

This paper presents a thermoporoelastic theory that allows for thermodynamically coupled fluid and heat flow, changing material properties, compressibility and thermal expansion of constituents, substantial temperature changes and convective heat flow. The model can be considered as a significant advancement of the models reported in the literature. The governing equations of the present model are first established and the underlying assumptions described. Reduction of the resulting non-linear governing equations to previous linearized models is shown for certain special cases. An exact analytical solution is presented for a one-dimensional soil column under the assumption of constant properties and a small change in temperature. The analytical solution is then used to demonstrate the significance of coupled effects. A finite element formulation is also presented. The accuracy of the finite element algorithm is established by comparison with the analytical solution. Selected non-linear finite element solutions for a one-dimensional soil column and a long cylindrical cavity are used to demonstrate the principal features of the coupled fields. Additional parametric studies are presented elsewhere (Zhou, 1998).

GOVERNING EQUATIONS

The present model makes the following assumptions. The porous medium is statistically isotropic. The fluid and solid phases are in thermal equilibrium. Small displacements and infinitesimal strains are assumed. The constitutive relationship for the solid skeleton is linearly elastic. [Solutions and numerical implementation for non-linear constitutive relations for the solid skeleton are well documented in the literature (Lubliner, 1990; Zienkiewicz, 1977)]. The medium is fully saturated and the fluid does not undergo a phase transformation.

Mechanical response

The constitutive relations of an isotropic linear poroelastic medium can be expressed in terms of the effective stress σ'_{ij} (positive for tension), strain ε_{ij} and temperature change T as

$$\sigma'_{ij} = 2G\left(\varepsilon_{ij}+\delta_{ij}\frac{v}{1-2v}\varepsilon_{kk}\right)-K'\alpha T\delta_{ij} \tag{1}$$

where $\sigma'_{ij} = \sigma_{ij}+\xi p\delta_{ij}$ and σ_{ij} denotes total stress (positive for tension), δ_{ij} is Kronecker's delta, p is pore water pressure (negative for suction), $\xi(\leqslant 1)$ is a coefficient which depends on the compressibility of the constituents $[\xi = 1-(K'/K_s)]$, K_s is bulk modulus of soil grains, $K'\{[= [2G(1+v)/3(1-2v)]\}$ is the drained bulk modulus of the soil medium, v is the drained Poisson's ratio, α is coefficient of volumetric expansion of soil medium ($^\circ C^{-1}$) and G is shear modulus of soil medium.

The equations of equilibrium and the strain–displacement relations can be expressed as

$$\sigma_{ij,j}+b_j = 0 \tag{2}$$

and

$$\varepsilon_{ij} = \tfrac{1}{2}(u_{i,j}+u_{j,i}) \tag{3}$$

respectively. Where b_i and u_i $(i = x, y, z)$ denote the net body force and displacement in the i-direction.

Equations (1)–(3) can be combined to obtain the following governing equation for displacement of the medium under a combination of changes of applied stresses, pore water pressures, and temperatures.

$$G\nabla^2 u_i + \frac{G}{1-2v} u_{j,ji} - \xi p_{,i} - K'\alpha T_{,i} + b_i = 0 \tag{4}$$

In the absence of pore water pressure and temperature gradients, eqn (4) reduces to the classical Navier equations for an ideal elastic solid.

Fluid flow

Consider a saturated soil element of volume V that consists of a volume V_s of soil grains and a volume V_e of voids. The rate of change of V, V_s and V_e with respect to the time (t) satisfies the following relationship

$$\frac{1}{V}\frac{\partial V}{\partial t} = \frac{1}{V}\frac{\partial V_e}{\partial t} + \frac{1}{V}\frac{\partial V_s}{\partial t} = \frac{\partial \varepsilon_v}{\partial t} \tag{5}$$

where ε_v is the volume strain.

The change of volume of soil grains is given by

$$\frac{1}{V}\frac{\partial V_s}{\partial t} = (1-n)a_s\frac{\partial T}{\partial t} - \frac{1-n}{K_s}\frac{\partial p}{\partial t} + \frac{1}{3K_s}\mathbf{m}\frac{\partial \boldsymbol{\sigma}'}{\partial t} \tag{6}$$

and

$$\mathbf{m} = \langle 1 \quad 1 \quad 1 \quad 0 \quad 0 \quad 0 \rangle \tag{7}$$

where n, a_s, and $\boldsymbol{\sigma}'$ denote the porosity (V_e/V), coefficient of volumetric thermal expansion of soil grains and effective stress vector, respectively. The three terms on the right-hand side of eqn (6) represent the volume change of soil grains due to changes of temperature, water pressure, and effective stresses, respectively.

The volume change of voids is given by

$$\frac{1}{V}\frac{\partial V_e}{\partial t} = -\nabla q_w + na_w\frac{\partial T}{\partial t} - \frac{n}{\beta_w}\frac{\partial p}{\partial t} \tag{8}$$

where q_w, a_w, and β_w denote the water flux/unit area (m/s), coefficient of thermal expansion (volume) and bulk modulus of pore water. The first term on the right hand side of eqn (8) represents the net volume of water flow out of the element, while the remaining two terms represent the volume change of water caused by changes of temperature and pore water pressure, respectively.

Substitution of eqns (6) and (8) into eqn (5) results in,

$$\nabla q_w = -\frac{\partial \varepsilon_v}{\partial t} + [na_w + (1-n)a_s]\frac{\partial T}{\partial t} - \left(\frac{n}{\beta_w} + \frac{1-n}{K_s}\right)\frac{\partial p}{\partial t} + \frac{1}{3K_s}\mathbf{m}\frac{\partial \boldsymbol{\sigma}'}{\partial t} \tag{9}$$

A quantitative description of thermodynamically coupled transport processes can be obtained from thermodynamics of irreversible processes (Fitts, 1962; Onsager, 1931). In this formulation, each flow (in the present case water and heat) in an open system supporting irreversible processes is written as a linear function of all forces acting within the system. Therefore water flux is given by the following equation

$$q_w = -k\nabla(p+\gamma_w z)+S_w\nabla T \tag{10}$$

where z is the vertical coordinate, k is the coefficient of permeability [$m^5/(Js)$] associated with Darcy flow; γ_w is specific weight of the pore water (N/m^3) and S_w is a phenomenological coefficient [$m^2/(s°C)$] associated with the influence of thermal gradient on the water flux (thermo-osmosis). Thermo-osmosis effects may significantly contribute to mass transfer in semi-impermeable clays (Carnahan, 1984). The gravity potential term in eqn (10) can be neglected without loss of any generality.

Substitution of eqns (10) and (1) in eqn (9) results in

$$\nabla(k\nabla p+S_w\nabla T) = c_1\frac{\partial u_{j,j}}{\partial t}-c_2\frac{\partial T}{\partial t}+c_3\frac{\partial p}{\partial t} \tag{11}$$

where

$$c_1 = 1-\frac{K'}{K_s};\quad c_2 = na_w+(1-n)a_s-\frac{\alpha K'}{K_s};\quad c_3 = \frac{n}{\beta_w}+\frac{1-n}{K_s} \tag{12}$$

For a medium with incompressible constituents (that is, $K_s, \beta_w \to \infty$), $c_1 = 1$, $c_2 = na_w+(1-n)a_s$ and $c_3 = 0$. (This condition also applies to cases where the compressibility of the constituents is much less than the compressibility of the soil medium.) If the thermo-osmosis effect is also neglected ($S_w = 0$), then the eqn (11) is identical to the fluid continuity equation presented by Seneviratne *et al.* (1994). For incompressible constituents in the absence of temperature effects and $S_w = 0$, eqns (4) and (11) are equivalent to the governing equations used by McNamee and Gibson (1960) for poroelasticity.

Heat flow

Jumikis (1966) and Farouki (1986) pointed out that the thermal conductivity of soil grains is one to five times that of water. Therefore, moisture content (that is, a measure of porosity) of a saturated soil has a great influence on thermal conductivity (λ) which varies with dry density and porosity. It is also noted that the gravimetric specific heat of soil grains and water are nearly constant. A coupled thermoporoelastic theory should take these factors into consideration.

The total heat flux q_T is given by

$$q_T = \rho_w q_w C_w T-\lambda\nabla T-S_w^*\nabla p \tag{13}$$

where

$$\lambda = (1-n)\lambda_s+n\lambda_w \tag{14}$$

and λ_s and λ_w are thermal conductivities of soil grain and water [$J/(s\cdot m\cdot °C)$]; C_w is the gravimetric specific heat of water ($J/kg/°C$); ρ_w is the density of water (kg/m^3); λ is the thermal conductivity of soil medium [$J/(s\cdot m\cdot °C)$] which is a function of porosity (therefore, a function of volume strain, pore water pressure and temperature) and S_w^* is a phenomenological coefficient associated with the contribution of the water pressure gradient to the heat flux (i.e., the thermal-filtration) arising from thermodynamically coupled transport processes. It can be shown that $S_w^* = (T+T_0)S_w$ where T_0 is the absolute reference temperature. The first term in eqn (13) represents the convective heat flux. If the convective heat transfer is neglected and $S_w^* = 0$, then the eqn (13) reduces to the classical Fourier law.

Due to the assumption of thermal equilibrium between the fluid and solid phases, the heat energy balance equation for the medium can be expressed in terms of a single equation of the following form

$$\frac{\partial[(V_s\rho_sC_s+V_e\rho_wC_w)T]}{V\partial t}-(T_0+T)a_w\beta_w\nabla q_w-(T_0+T)K'\alpha\frac{\partial\varepsilon_v}{\partial t}=-\nabla q_T \tag{15}$$

The first term on the left-hand side of eqn (15) represents the rate of internal heat energy change per unit volume due to an increase in temperature. The second term represents a heat sink due to thermal dilatation of the fluid. Biot (1956) neglected this term and it is included here for completeness. The last term on the left-hand side of eqn (15) represents a heat sink due to thermal expansion of the medium. For a small variation of temperature, $T_0+T\approx T_0$, this term is identical to that given by Biot (1956). The second and third term on the left-hand side of eqn (15) represent the thermoporoelastic coupling in the heat energy balance equation. The contribution due to other mechanical effects such as the conversion of strain energy into heat energy is neglected in the eqn (15). It is generally recognized that such contributions can be neglected for the present class of problems.

The conservation of mass of the two phases in the representative element yields,

$$\frac{\partial(V_s\rho_s)}{V\partial t}=0 \tag{16}$$

$$\frac{\partial(V_e\rho_w)}{V\partial t}=-\rho_w\nabla q_w \tag{17}$$

Equations (16) and (17) indicate that density changes of soil grains and water are always associated with a change of volume or porosity.

The density of water is a function of water pressure and temperature. The thermal conductivity depends on porosity, which, in turn, depends on stresses, water pressure and temperature. Assuming that the gravimetric specific heats (C_s, C_w) are constant, the eqn (15) can be expressed in the following form using eqns (13), (16) and (17)

$$C_v\frac{\partial T}{\partial t}-(T_0+T)K'\alpha\frac{\partial\varepsilon_v}{\partial t}=C_wTq_w\nabla\rho_w-\rho_wC_wq_w\nabla T+\lambda\nabla^2T+\nabla\lambda\nabla T+\nabla(S_w^*\nabla p)$$
$$-(T_0+T)a_w\beta_w\nabla(k\nabla p+S_w\nabla T) \tag{18}$$

where C_v is the volumetric specific heat of the soil medium (J/m^3/°C) which is given by

$$C_v=(1-n)\rho_sC_s+n\rho_wC_w \tag{19}$$

The equation of state for water is given by Fernandez (1972) as

$$\rho_w=\rho_{w0}\exp\left(-\alpha_wT+\frac{p}{\beta_w}\right) \tag{20}$$

where ρ_{w0} is the initial density of water.

By retaining the first order terms of the above equation, the gradient of density of water can be expressed in terms of gradients of water pressure and temperature as,

$$\nabla\rho_w\approx\rho_{w0}\left(-\alpha_w\nabla T+\frac{1}{\beta_w}\nabla p\right) \tag{21}$$

Using the eqn (14), assuming that λ_w and λ_s are both constant, the gradient of thermal conductivity of the soil can be expressed by,

$$\nabla\lambda=(\lambda_w-\lambda_s)\nabla n \tag{22}$$

Substitution of eqns (21) and (22) into eqn (18) results in,

$$C_v\frac{\partial T}{\partial t}-(T+T_0)K'\alpha\frac{\partial \varepsilon_v}{\partial t}=(\lambda_w-\lambda_s)\nabla T\nabla n$$
$$+C_w\left[\rho_w k+\rho_{w0}T\left(-a_w k+\frac{S_w}{\beta_w}\right)\right]\nabla T\nabla p+\frac{\rho_{w0}C_w kT}{\beta_w}(\nabla p)^2$$
$$+C_w S_w(\rho_w-a_w\rho_{w0}T)(\nabla T)^2+\lambda\nabla^2 T+\nabla(S_w^*\nabla p)-(T+T_0)\alpha_w\beta_w\nabla(k\nabla p+S_w\nabla T) \quad (23)$$

The first term on the right-hand side represents the effect of porosity change, the second and third terms represent the linear and non-linear hydraulic effects, the fourth term represents non-linear temperature effect, the fifth term represents the classical heat conduction term, the sixth term represents the contribution due to thermal-filtration, and the last term is associated with convection.

The rate of change of porosity (n) can be expressed from the eqns (5) and (6) as

$$\frac{\partial n}{\partial t}=\left(1-\frac{K'}{K_s}\right)\frac{\partial \varepsilon_v}{\partial t}+\left[\frac{K'}{K_s}\alpha-(1-n)a_s\right]\frac{\partial T}{\partial t}+\frac{1-n}{K_s}\frac{\partial p}{\partial t} \quad (24)$$

Equations (4), (11) and (23) with porosity determined from eqn (24) represent a set of fully coupled non-linear equations governing the thermoporoelastic response of a saturated medium. The equations account for thermodynamically coupled heat-mass transfer, compressibility and thermal expansion of constituents, convective heat flow, relatively large variation of temperature ($T_0+T\neq T_0$) and porosity dependent soil properties (for example, density, thermal diffusivity, etc.). Depending on the significance of coupling between driving forces, type of soil, and other factors in a given problem, the theory can be reduced to obtain simpler governing equations.

The following sections simplify the theory to obtain a set of linear governing equations while retaining the principal coupling terms.

For small changes of porosity, eqn (24) can be approximated by

$$n\approx n_0+\left(1-\frac{K'}{K_s}\right)\varepsilon_v+\left[\frac{K'}{K_s}\alpha-(1-n_0)a_s\right]T+\frac{1-n_0}{K_s}p \quad (25)$$

where n_0 is the initial porosity.

The gradient of porosity can be expressed as

$$\nabla n=\left(1-\frac{K'}{K_s}\right)\nabla\varepsilon_v+\left[\frac{K'}{K_s}\alpha-(1-n_0)a_s\right]\nabla T+\frac{1-n_0}{K_s}p \quad (26)$$

Substitution of eqn (26) in eqn (23) results in the following energy balance equation

$$C_v\frac{\partial T}{\partial t}-(T+T_0)K'\alpha\frac{\partial \varepsilon_v}{\partial t}=(\lambda_w-\lambda_s)\left(1-\frac{K'}{K_s}\right)\nabla T\nabla\varepsilon_v$$
$$+\left\{(\lambda_w-\lambda_s)\left(\frac{1-n_0}{K_s}\right)+C_w\left[\rho_w k+\rho_{w0}T\left(-a_w k+\frac{S_w}{\beta_w}\right)\right]\right\}\nabla T\nabla p+\frac{\rho_{w0}C_w kT}{\beta_w}(\nabla p)^2$$
$$+\left\{(\lambda_w-\lambda_s)\left[\frac{K'}{K_s}\alpha-(1-n_0)a_s\right]+C_w S_w(\rho_w-a_w\rho_{w0}T)\right\}(\nabla T)^2$$
$$+\lambda\nabla^2 T+\nabla(S_w^*\nabla p)-(T+T_0)\alpha_w\beta_w\nabla(k\nabla p+S_w\nabla T) \quad (27)$$

Numerical studies indicate that the third term on the right-hand side of eqn (27) can be neglected for clayey materials ($k/\beta_w \approx 0$). Equations (4), (11) and (27) are a set of simplified non-linear governing equations for thermoporoelasticity.

Neglecting convective heat transfer, and assuming that (1) volumetric specific heat (C_v) is constant, (2) thermal conductivity (λ) is constant, and (3) the variation of temperature is relatively small ($T_0+T \approx T_0$), (4) $S_w^* = (T+T_0)S_w \approx T_0 S_w$, eqn (18) can be simplified as:

$$C_v \frac{\partial T}{\partial t} - T_0 K' \alpha \frac{\partial \varepsilon_v}{\partial t} = (\lambda - T_0 \alpha_w \beta_w S_w)\nabla^2 T + T_0(S_w - \alpha_w \beta_w k)\nabla^2 p \tag{28}$$

Equations (4), (11) and (28) are a set of linear governing equations for thermoporoelasticity. If further simplifications are made by neglecting the heat sink associated with dilatation of fluid and also thermodynamically coupled transport processes ($S_w = 0$), eqn (28) reduces to the following heat energy balance equation which is identical to the eqn (3.4) of Biot (1956).

$$C_v \frac{\partial T}{\partial t} - T_0 K' \alpha \frac{\partial \varepsilon_v}{\partial t} = \lambda \nabla^2 T \tag{29}$$

Equations (4), (11) and (29) with constant parameters c_1, c_2 and c_3 [eqn (12)] represent a set of coupled linear governing equations analogous to those reported in literature.

Due to the complexity of the coupling effects in this formulation, numerical methods such as the finite element method must be used to solve the governing eqns (4), (11), (23) and (24). To the author's knowledge, solutions have not previously been reported for a thermoporoelastic model with the coupling described by these equations. It is therefore important to first derive an analytical solution for a relatively simple linear case in which the nonlinearities in the coupled model have been relaxed. Such a solution is useful for two purposes. First it assists in checking the accuracy of the finite element solutions developed for the more general case with non-linear governing equations. Secondly it provides some insight into the significance of the coupling effects described by various terms and in the estimation of the influence of various material parameters without elaborate computational work.

ANALYTICAL SOLUTION

This section derives an analytical solution for a laterally confined one-dimensional column of soil. The top end of the column is fully permeable and subjected to a compressive stress σ_0 and a constant temperature increase T_1. The fully permeable bottom end is fixed and kept at T_0. All material parameters are assumed to be constant, and convective heat-transfer is neglected. Temperature increase is assumed to be relatively small.

From eqns (4), (11) and (28) the governing equations for the simplified 1-D problem can be expressed in terms of the basic unknowns $\varepsilon_v(x,t)$, $p(x,t)$, and $T(x,t)$

$$\frac{1-v}{1-2v} 2G \frac{\partial^2}{\partial x^2} \varepsilon_v - \xi \frac{\partial^2}{\partial x^2} p - K' \alpha \frac{\partial^2}{\partial x^2} T = 0 \tag{30}$$

$$k \frac{\partial^2}{\partial x^2} p + S_w \frac{\partial^2}{\partial x^2} T = c_1 \frac{\partial \varepsilon_v}{\partial t} - c_2 \frac{\partial T}{\partial t} + c_3 \frac{\partial p}{\partial t} \tag{31}$$

$$C_v \frac{\partial T}{\partial t} - T_0 K' \alpha \frac{\partial \varepsilon_v}{\partial t} = (\lambda - T_0 \alpha_w \beta_w S_w) \frac{\partial^2}{\partial x^2} T + T_0 (S_w - \alpha_w \beta_w k) \frac{\partial^2}{\partial x^2} p \tag{32}$$

where $\varepsilon_v = (\partial u_x / \partial x)$ and u_x is the displacement in the x-direction.

The boundary conditions can be expressed as

$$\sigma_{xx}(0,t) = -\sigma_0\,; \quad p(0,t) = 0\,; \quad T(0,t) = T_1\,; \quad u_x(l,t) = 0\,; \quad p(l,t) = 0\,; \quad T(l,t) = 0 \tag{33}$$

and the initial conditions are,

$$\sigma_{xx}(x,0) = 0\,; \quad p(x,0) = 0\,; \quad T(x,0) = 0 \tag{34}$$

The details of the solution of eqns (30)–(32) subject to the above boundary and initial conditions are presented in the Appendix A. The following time-domain solutions are obtained for pore pressure (p), temperature (T) and the displacement (u_x)

$$\begin{aligned}
p = &-\frac{T_1}{h_1(\gamma_1^2-\gamma_2^2)}\left\{\sum_{m=0}^{\infty}\left[\operatorname{erfc}\frac{[(2m+2)l-x]\gamma_1}{2\sqrt{t}} - \operatorname{erfc}\frac{[2ml+x]\gamma_1}{2\sqrt{t}}\right.\right.\\
&\left.-\operatorname{erfc}\frac{[(2m+2)l-x]\gamma_2}{2\sqrt{t}} + \operatorname{erfc}\frac{[2ml+x]\gamma_2}{2\sqrt{t}}\right]\Bigg\}\\
&+\frac{\sigma_0}{h_1(\gamma_1^2-\gamma_2^2)}\left\{(h_3-h_0h_1\gamma_2^2)\left[\operatorname{erfc}\frac{(l-x)\gamma_1}{2\sqrt{t}} + \sum_{m=0}^{\infty}(-1)^m\left[\operatorname{erfc}\frac{(2ml+x)\gamma_1}{2\sqrt{t}}\right.\right.\right.\\
&\left.-\operatorname{erfc}\frac{[(2m+1)l+x]\gamma_1}{2\sqrt{t}} - \operatorname{erfc}\frac{[(2m+2)l-x]\gamma_1}{2\sqrt{t}} + \operatorname{erfc}\frac{[(2m+3)l-x]\gamma_1}{2\sqrt{t}}\right]\Bigg]\\
&-(h_3-h_0h_1\gamma_1^2)\left[\operatorname{erfc}\frac{(l-x)\gamma_2}{2\sqrt{t}} + \sum_{m=0}^{\infty}(-1)^m\left[\operatorname{erfc}\frac{(2ml+x)\gamma_2}{2\sqrt{t}}\right.\right.\\
&\left.\left.\left.-\operatorname{erfc}\frac{[(2m+1)l+x]\gamma_2}{2\sqrt{t}} - \operatorname{erfc}\frac{[(2m+2)l-x]\gamma_2}{2\sqrt{t}} + \operatorname{erfc}\frac{[(2m+3)l-x]\gamma_2}{2\sqrt{t}}\right]\right]\right\} - h_0\sigma_0
\end{aligned} \tag{35}$$

$$\begin{aligned}
T = &-\frac{T_1}{h_1(\gamma_1^2-\gamma_2^2)}\sum_{m=0}^{\infty}\left\{(h_1\gamma_1^2+h_2)\left[\operatorname{erfc}\frac{[(2m+2)l-x]\gamma_1}{2\sqrt{t}} - \operatorname{erfc}\frac{[2ml+x]\gamma_1}{2\sqrt{t}}\right]\right.\\
&\left.-(h_1\gamma_2^2+h_2)\left[\operatorname{erfc}\frac{[(2m+2)l-x]\gamma_2}{2\sqrt{t}} - \operatorname{erfc}\frac{[2ml+x]\gamma_2}{2\sqrt{t}}\right]\right\}\\
&+\frac{\sigma_0}{h_1(\gamma_1^2-\gamma_2^2)}\left\{(h_3-h_0h_1\gamma_2^2)(h_1\gamma_1^2+h_2)\left[\operatorname{erfc}\frac{(l-x)\gamma_1}{2\sqrt{t}} + \sum_{m=0}^{\infty}(-1)^m\left[\operatorname{erfc}\frac{(2ml+x)\gamma_1}{2\sqrt{t}}\right.\right.\right.\\
&\left.-\operatorname{erfc}\frac{[(2m+1)l+x]\gamma_1}{2\sqrt{t}} - \operatorname{erfc}\frac{[(2m+2)l-x]\gamma_1}{2\sqrt{t}} + \operatorname{erfc}\frac{[(2m+3)l-x]\gamma_1}{2\sqrt{t}}\right]\Bigg]\\
&-(h_3-h_0h_1\gamma_1^2)(h_1\gamma_2^2+h_2)\left[\operatorname{erfc}\frac{(l-x)\gamma_2}{2\sqrt{t}} + \sum_{m=0}^{\infty}(-1)^m\left[\operatorname{erfc}\frac{(2ml+x)\gamma_2}{2\sqrt{t}}\right.\right.\\
&\left.\left.\left.-\operatorname{erfc}\frac{[(2m+1)l+x]\gamma_2}{2\sqrt{t}} - \operatorname{erfc}\frac{[(2m+2)l-x]\gamma_2}{2\sqrt{t}} + \operatorname{erfc}\frac{[(2m+3)l-x]\gamma_2}{2\sqrt{t}}\right]\right]\right\}\\
&-(h_0h_2+h_3)\sigma_0
\end{aligned} \tag{36}$$

$$\begin{aligned}
u_x = &-\frac{T_1}{h_1(\gamma_1^2-\gamma_2^2)}\sum_{m=0}^{\infty}(-1)^m\left\{-\frac{E_1}{\gamma_1}[\phi\langle[(2m+2)l-x]\gamma_1\rangle - \phi\langle(2m+1)l\gamma_1\rangle]\right.\\
&-\frac{F_1}{\gamma_1}[\phi\langle(2ml+x)\gamma_1\rangle - \phi\langle(2m+1)l\gamma_1\rangle] \quad \left.+\frac{E_2}{\gamma_2}[\phi\langle[(2m+2)l-x]\gamma_2\rangle - \phi\langle(2m+1)l\gamma_2\rangle]\right.
\end{aligned}$$

$$+\frac{F_2}{\gamma_2}[\phi\langle(2ml+x)\gamma_2\rangle-\phi\langle(2m+1)l\gamma_2\rangle]\Bigg\}$$

$$+\frac{\sigma_0}{h_1(\gamma_1^2-\gamma_2^2)}\Bigg\{(h_3-h_0h_1\gamma_2^2)\frac{E_1}{\gamma_1}[\phi\langle(l-x)\gamma_1\rangle-\phi\langle 0\rangle]$$

$$-(h_3-h_0h_1\gamma_1^2)\frac{E_2}{\gamma_2}[\phi\langle(l-x)\gamma_2\rangle-\phi\langle 0\rangle]\Bigg\}$$

$$-\sum_{m=0}^{\infty}(-1)^m\Bigg\{(h_3-h_0h_1\gamma_2^2)\Bigg[\frac{E_1}{\gamma_1}[\phi\langle[(2m+2)l-x]\gamma_1\rangle-\phi\langle[(2m+3)l-x]\gamma_1\rangle$$

$$-\phi\langle(2m+1)l\gamma_1\rangle+\phi\langle(2m+2)l\gamma_1\rangle]+\frac{F_1}{\gamma_1}[\phi\langle(2ml+x)\gamma_1\rangle-\phi\langle[(2m+1)l+x]\gamma_1\rangle$$

$$-\phi\langle(2m+1)l\gamma_1\rangle+\phi\langle(2m+2)l\gamma_1\rangle\Bigg]$$

$$-(h_3-h_0h_1\gamma_1^2)\Bigg[\frac{E_2}{\gamma_2}[\phi\langle[(2m+2)l-x]\gamma_2\rangle-\phi\langle[(2m+3)l-x]\gamma_2\rangle$$

$$-\phi\langle(2m+1)l\gamma_2\rangle+\phi\langle(2m+2)l\gamma_2\rangle]+\frac{F_2}{\gamma_2}[\phi\langle(2ml+x)\gamma_2\rangle-\phi\langle((2m+1)l+x)\gamma_2\rangle$$

$$-\phi\langle(2m+1)l\gamma_2\rangle+\phi\langle(2m+2)l\gamma_2\rangle\Bigg]\Bigg\}-f\sigma_0(x-l) \tag{37}$$

and

$$\phi\langle x\rangle = 2\sqrt{\frac{t}{\pi}}e^{-x^2/4t}-x\,\mathrm{erfc}\frac{x}{2\sqrt{t}}$$

where erfc(x) denotes the complementary error function of argument x (Abramowitz and Stegun, 1965). γ_1, γ_2, E_1, E_2, F_1, F_2, and h_i, $i = 0, \ldots, 3$ are defined in Appendix A.

FINITE ELEMENT FORMULATION

The coupled non-linear response described by eqns (4), (11), (23) and (24) can only be solved numerically, for example, using the finite element method. This section presents a mixed finite element formulation of the new thermoporoelastic model. In the absence of body forces, the equilibrium eqn (4) can be replaced by the following equation of virtual work

$$\int_\Omega \delta\boldsymbol{\varepsilon}^T\boldsymbol{\sigma}\,\mathrm{d}\Omega-\int_S \delta\mathbf{u}^T\mathbf{t}\,\mathrm{d}S = 0 \tag{38}$$

where $\mathbf{u}$, $\boldsymbol{\varepsilon}$, $\boldsymbol{\sigma}$ and $\mathbf{t}$ denote displacement, strain, stress, and surface traction vectors.

The Galerkin method (Zienkiewicz, 1977) is introduced to obtain finite element representations of the eqns (11), (23) and (24) that include first order time derivatives. In this mixed formulation, displacements, pore water pressure, temperature and porosity are interpolated as,

$$\mathbf{u}(t) = \mathbf{N}_u\hat{\mathbf{U}}(t)\,;\quad \mathbf{p}(t) = \mathbf{N}_p\hat{\mathbf{P}}(t)\,;\quad \mathbf{T}(t) = \mathbf{N}_T\hat{\mathbf{T}}(t)\,;\quad \mathbf{n}(t) = \mathbf{N}_n\hat{\mathbf{n}}(t)\,; \tag{39}$$

where $\hat{\mathbf{U}}(t)$, $\hat{\mathbf{P}}(t)$, $\hat{\mathbf{T}}(t)$ and $\hat{\mathbf{n}}(t)$ are vectors of nodal displacements, pore water pressure,

temperature and porosity at time t; $\mathbf{N}_u$, $\mathbf{N}_p$, $\mathbf{N}_T$ and $\mathbf{N}_n$ are matrices of shape functions for displacement, pore water pressure, temperature and porosity, respectively.

Equations (11) and (23) can be reformulated by introducing eqn (24) in order to eliminate the mixed derivatives of displacements on their left-hand side. By using eqn (24), the water continuity eqn (11) is rewritten as

$$\frac{n}{\beta_w}\frac{\partial p}{\partial t} - na_w\frac{\partial T}{\partial t} + \frac{\partial n}{\partial t} = \nabla(k\nabla p + S_w\nabla T) \tag{40}$$

In view of eqns (24) and (40), the heat energy balance eqn (23) can be then rewritten as

$$\zeta_1\frac{\partial p}{\partial t} + \zeta_2\frac{\partial T}{\partial t} + \zeta_3\frac{\partial n}{\partial t} = (\lambda_w - \lambda_5)\nabla T\nabla n + \zeta_4\nabla T\nabla p + \zeta_5(\nabla p)^2 + \zeta_6(\nabla T)^2 + \lambda\nabla^2 T + \nabla(S_w^*\nabla p) \tag{41}$$

where ζ_i ($i = 1, \ldots, 6$) are defined in Appendix B.

Equations (38), (40), (41) and (24) are used as the governing equations in the finite element formulation. (Note that they are fully analogous to eqns (4), (11), (23) and (24).) A quadratic shape function is chosen in the current finite element analysis with $\mathbf{N}_u = \mathbf{N}_p = \mathbf{N}_T = \mathbf{N}_n = \mathbf{N}$. The substitution of eqn (39) into eqn (1) and (3) results in

$$\boldsymbol{\varepsilon} = \mathbf{B}\hat{\mathbf{U}}(t) \tag{42}$$

$$\boldsymbol{\sigma} = \mathbf{DB}\hat{\mathbf{U}}(t) - \xi\mathbf{m}^T\mathbf{N}\hat{\mathbf{P}}(t) - K'\alpha\mathbf{m}^T\mathbf{N}\hat{\mathbf{T}}(t) \tag{43}$$

where $\mathbf{B}$ is strain shape function matrix and $\mathbf{D}$ is the constitutive matrix.

The substitution of eqn (39), (42) and (43) into eqn (38), and the application of Galerkin method to eqns (40), (41) and (24) with $\mathbf{N}$ as the weight function results in

$$\mathbf{G}\dot{\mathbf{X}} + \mathbf{KX} = \mathbf{F} \tag{44}$$

The coefficient matrices $\mathbf{G}$ and $\mathbf{K}$ are given in the Appendix B, and depend on the nodal unknowns. There are numerous methods for solving this kind of non-linear equation. In the present study, a backward difference time-stepping scheme is adopted. This offers the following advantages (Lewis and Schrefler, 1987): (1) it can solve for the time t_{i+1}, by evaluating the coefficient matrices at time t_i thus avoiding an iterative solution procedure; (2) it is found to reduce oscillations that appear in solving thermal problems with convective boundary conditions. The following manipulation (Noorishad *et al.*, 1984) is used to obtain a fully implicit one-step direct solution of the eqn (44):

$$\begin{aligned}\nabla T\nabla p &= \tfrac{1}{2}\nabla T_i\nabla p_{i+1} + \tfrac{1}{2}\nabla p_i\nabla T_{i+1}\\ n\nabla T &= \tfrac{1}{2}n_i\nabla T_{i+1} + \tfrac{1}{2}\nabla T_i n_{i+1}\end{aligned} \tag{45}$$

where i refers to the time level t_i.

Considering a time interval of Δt, the eqn (44) can be rewritten in the following incremental form

$$(\mathbf{G}_i + \Delta t\mathbf{K}_i)\Delta\mathbf{X} = \Delta t(\mathbf{F}_i - \mathbf{K}_i\mathbf{X}_i) \tag{46}$$

The subscript i refers to the time instant t_i, while $\Delta t(=t_{i+1}-t_i)$ refers to the time step and $\Delta\mathbf{X} = \mathbf{X}_{i+1} - \mathbf{X}_i$ refers to the incremental nodal variable vector. Equation (46) can be solved by starting from the initial solution with appropriate boundary conditions to obtain the nodal variables corresponding to various time instances. A constant Δt has been used in

the present study. Zienkiewicz (1977) and Lewis and Schrefler (1987) present details of the solution of time-dependent finite element equations including the stability of the time-stepping schemes.

NUMERICAL RESULTS

A computer code based on the above formulation has been developed. At every time step in the transient analysis, the porosity, thermal conductivity and volumetric specific heat are updated using eqns (24), (14) and (19). The density of water and soil grains are updated using the following relations

$$\rho_w = \rho_{w0}\left(1+\frac{p}{\beta_w}-a_w T\right) \tag{47}$$

$$\rho_s = \rho_{s0}\left[1+\frac{1-n}{K_s}p-(1-n)a_s T-\frac{K'}{K_s}(\varepsilon_v-\alpha T)\right] \tag{48}$$

where ρ_{w0} and ρ_{s0} are initial values of water and soil grain density, respectively. The eqn (48) is obtained by using eqns (6) and (1).

The permeability of soil is updated by using the following relationship (Carman, 1937)

$$\frac{k}{k_0}=\left(\frac{n}{n_0}\right)^3\left(\frac{1-n_0}{1-n}\right)^2\left(\frac{\mu_0}{\mu}\right) \tag{49}$$

where μ is the kinematic viscosity of water, k_0 is the initial value of permeability, μ_0 is the initial value of kinematic viscosity of water, and n_0 is the initial porosity. The kinematic viscosity (μ) which is a function of temperature is linearly interpolated from properties given by Chapman (1967).

A selected set of numerical results is presented in this section to demonstrate the significance of the thermodynamically coupled transport processes and the essential features of the coupled non-linear response computed using the finite element analysis. Two sets of material properties (material A and material B) are used in the analysis. The material properties given below are the same for both materials

$$a_w = 3.0\times10^{-4}{}^\circ\mathrm{C}^{-1},\quad a_s = 3.0\times10^{-6}{}^\circ\mathrm{C}^{-1},$$
$$\alpha = 3.0\times10^{-6}{}^\circ\mathrm{C}^{-1},\quad T_0 = 300\ \mathrm{K}$$
$$C_s = 0.937\ (\mathrm{kJ/kg/^\circ C}),\quad C_w = 4.186\ (\mathrm{kJ/kg/^\circ C}),$$
$$\rho_{w0} = 1000\ \mathrm{kg/m^3},\quad \rho_{s0} = 2610\ \mathrm{kg/m^3},$$
$$\beta_w = 3.3\ \mathrm{GPa},\quad K_s = 59\ \mathrm{GPa}$$
$$\lambda_s = 3.29\ \mathrm{J/(s\cdot m\cdot ^\circ C)},\quad \lambda_w = 0.582\ \mathrm{J/(s\cdot m\cdot ^\circ C)}$$

In addition for material A,

$$S_w = 6.0\times10^{-11}\ \mathrm{m^2/(s^\circ C)}\quad k_0 = 1.0\times10^{-14}\ \mathrm{m^5/(Js)}$$
$$E = 5.0\ \mathrm{MPa},\quad \nu = 0.2,\quad n_0 = 0.25$$

and for material B,

$$S_w = 2.70\times10^{-10}\ \mathrm{m^2/(s^\circ C)}\quad k_0 = 5.0\times10^{-14}\ \mathrm{m^5/(Js)}\quad \text{(Carnahan, 1984)}$$
$$E = 2.880\ \mathrm{MPa},\quad \nu = 0.2,\quad n_0 = 0.375$$

Figure 1 shows the response of a thermodynamically coupled soil column (material A) of 5 m length with fully drained ends subjected to sudden heating at the top end ($T = 50°C$ at $x = 0$ and $T = 0°C$ at $x = 5$ m) at seven different time instants. The column is fixed at the bottom end and stress free at the top end. The initial conditions are given by eqn (34). The properties of the column are constant and the response is computed by using eqns (35)–(37). Figure 2 shows the response of an identical column in the absence of thermodynamically coupled heat–water flow ($S_w = 0$). Comparison of Figs 1 and 2 indicates that substantial pore water pressure is developed in the column due to thermodynamically coupled heat–mass transfer. For example, the maximum pore water pressure in Fig. 1 is approximately 25 kPa when compared to 15 kPa in Fig. 2. The general shapes of the pore water pressure isochrones are identical for both cases. Pore water pressure is initially generated near the heated end and propagates along the column as time progresses. The time for complete dissipation of pore water pressure is more than 50,000 h.

The isochrones of temperature change shown in Figs 1 and 2 are identical. This means that the thermo-osmosis and thermal-filtration have negligible influence on the temperature distribution in the column. Temperatures reach their steady-state linear distribution well ahead of the complete pore water pressure dissipation. Thus, as is found in laboratory and field scale experiments, temperature fields are much easier to measure and calculate than displacement or pore water pressure fields (Graham *et al.*, 1996). However, the isochrones for displacements shown in Figs 1 and 2 show substantial differences. In both cases the column expands longitudinally for some time after first heating and then starts to shrink. This is because the water and soil skeleton expand initially due to heating causing local increases in pore water pressure. With time, water drains out from the ends, the excess pore water pressures decrease, and the decreases in water content result in a reduction in the expansion. The steady-state displacement distribution of the column in this example is linear, with maximum displacement at the heated end at all times. The peak displacements are about 7 mm in the thermodynamically uncoupled case (Fig. 2) and about 12.6 mm for the thermodynamically coupled case (Fig. 1). The peak displacement for the thermodynamically uncoupled case ($S_w = 0$) is smaller than the coupled case at all times, although the steady-state value is identical for both cases.

Figure 3 shows the response of a 5 m long soil column of material B subjected to the same boundary and initial conditions as in Figs 1 and 2. Material B has higher values of S_w and k_0. It is softer and less dense than material A. The coupled analytical solution [eqns (35)–(37)] for pore water pressure and displacement in Fig. 3 are substantially different from that in Figs 1 and 2. Pore water pressures are higher in Fig. 3 but also dissipate more rapidly (note the higher S_w, k_0 and n_0 for material B). The temperature isochrones in Fig. 3 are relatively closer to those in Figs 1 and 2. This implies only a minor dependence of temperature on parameters S_w and k_0. The displacements in Fig. 3 are relatively larger than those in Figs 1 and 2. The reason for this is that material B contains more water than material A and therefore expands more under heating. The steady-state solution is identical to that in Figs 1 and 2. Figure 3 also shows a comparison of the analytical solution with the finite element solution. The agreement is excellent and the finite element solution remains stable with increasing time. The porosity and other soil parameters are kept constant in the finite element analysis to be consistent with the analytical solutions.

Figure 4 shows the finite element solution for the same soil column but now taking account of changes of soil properties as given by eqns (14), (19), (25), (47), (48) and (49). This set of solutions corresponds to the new non-linear governing equations developed in this study. Solutions were computed for $\Delta t = 0.5$, 1.0 and 2.0 h to check the convergence and stability of the finite element solutions. Negligible differences were found between solutions corresponding to different Δt values. Comparison of Figs 3 and 4 indicates that both pore water pressure and displacement from the non-linear coupled model are lower than the linear coupled model. For example, the peak pore water pressure and displacement of the non-linear model are 25 kPa and 22 mm, respectively, compared to corresponding values of 35 kPa and 33 mm from the linear model. There are small differences between the temperature distributions calculated using the linear and non-linear models in this problem. Steady-state of basic variables is reached faster in the non-linear model. This is primarily

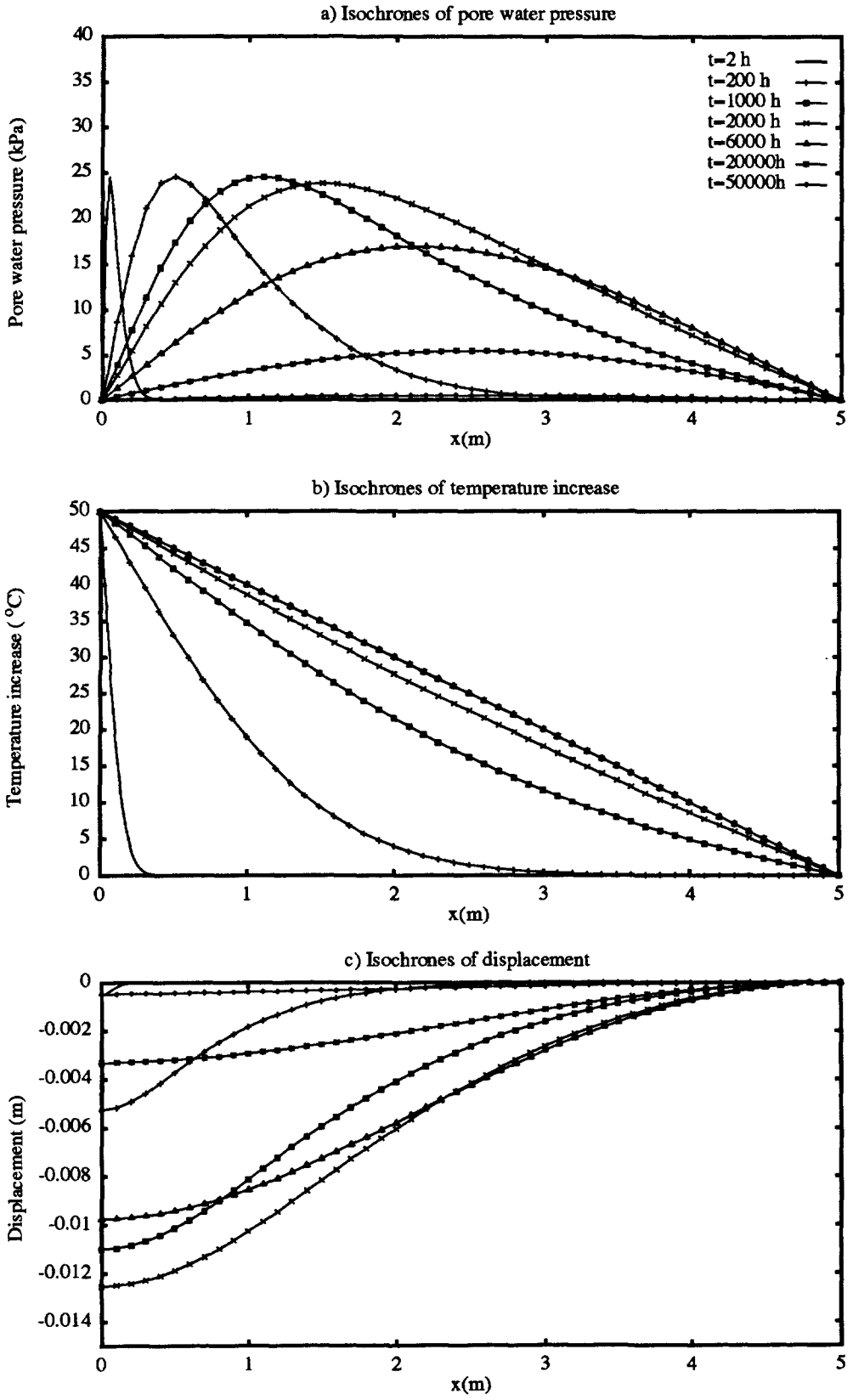

Fig. 1. Coupled analytical solution of a heated soil column with constant properties (material A).

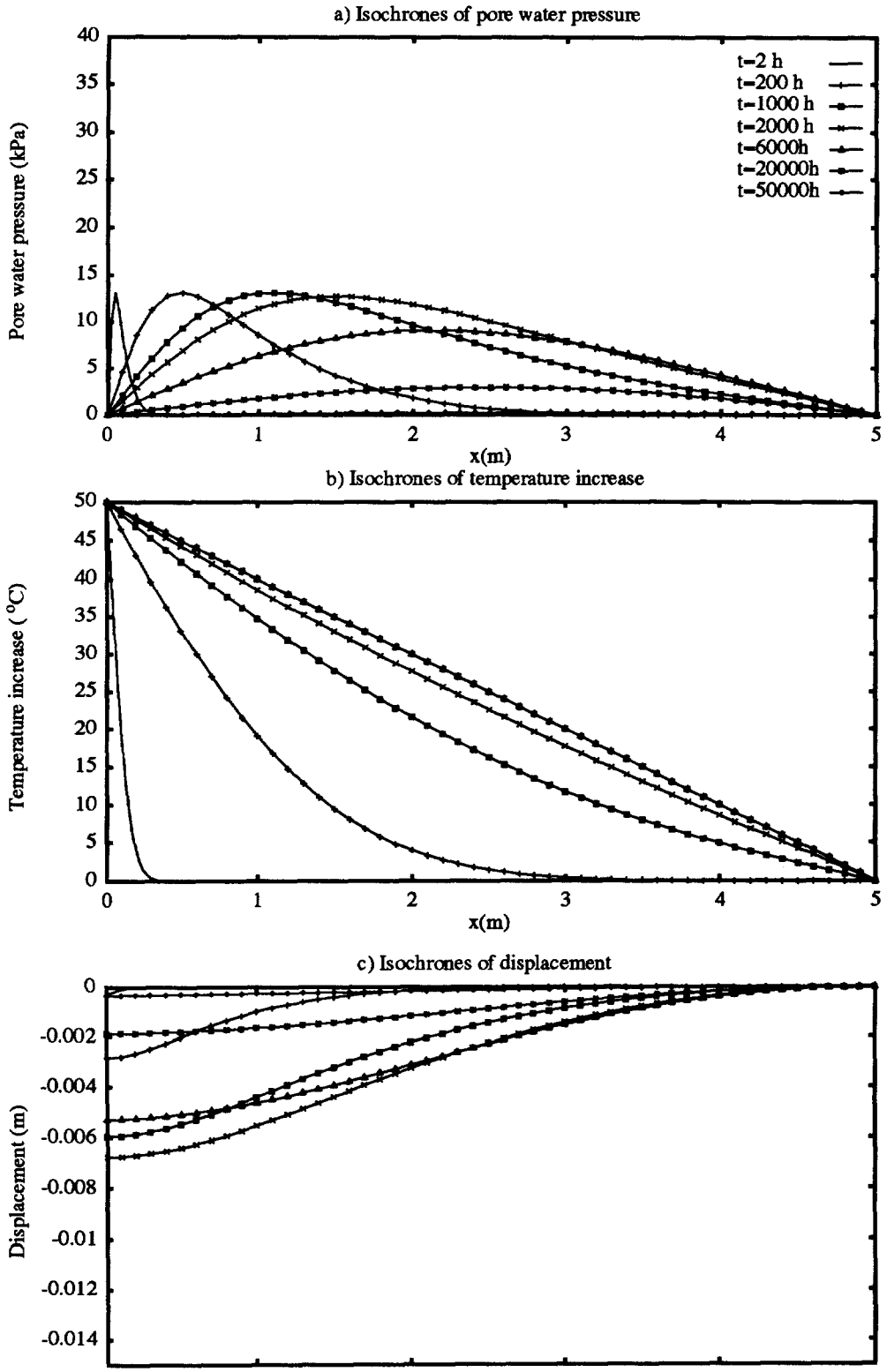

Fig. 2. Semi-coupled analytical solution ($S_w = 0$) of a heated soil column with constant properties (material A).

due to increases in permeability arising from decreases of dynamic viscosity produced by heating. The increase in permeability also causes water to flow out relatively earlier from the ends thus reducing the peak value of the displacements.

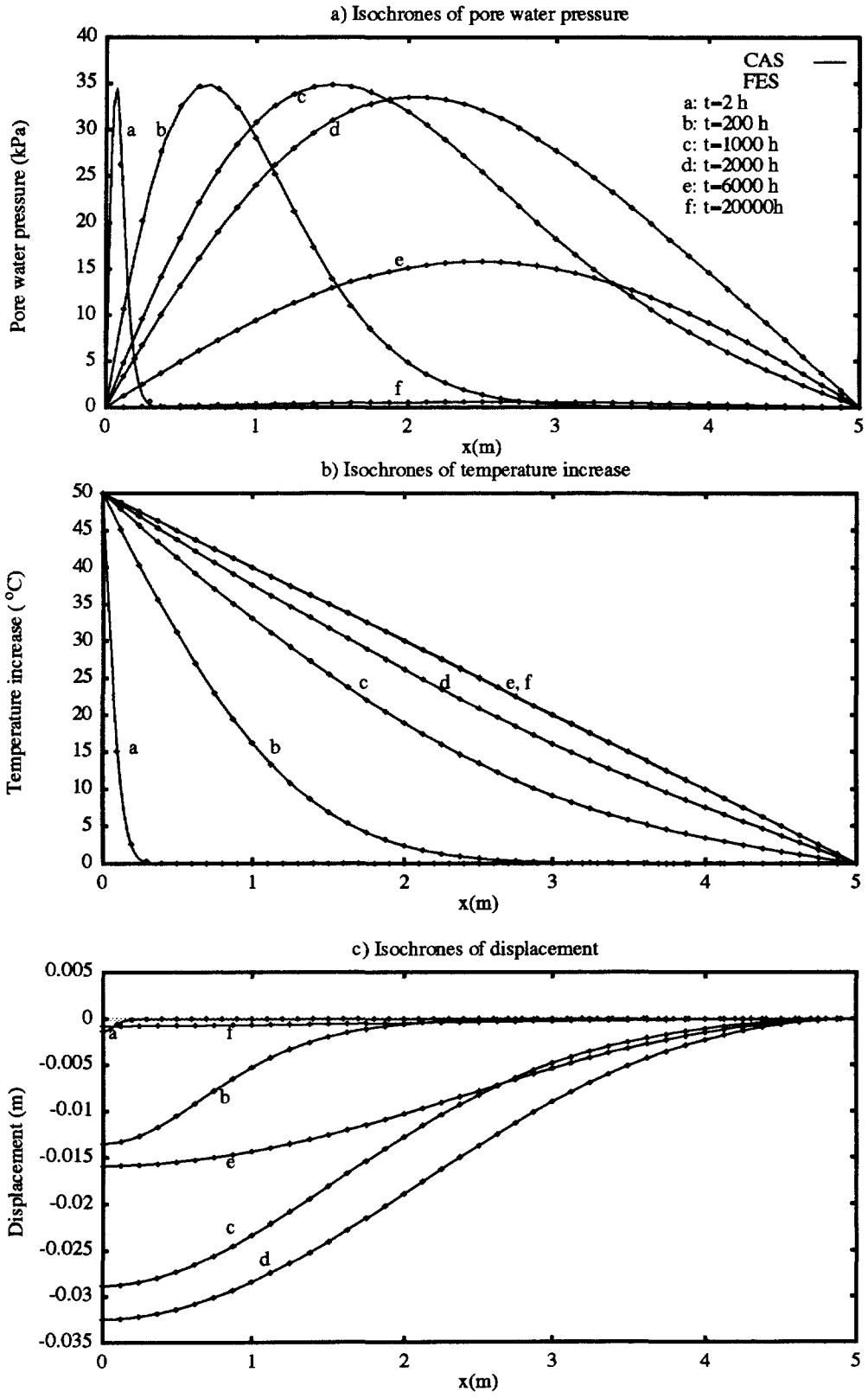

Fig. 3. Coupled analytical solution (CAS) and finite element solutions (FES) of a heated soil column with constant material properties (material B).

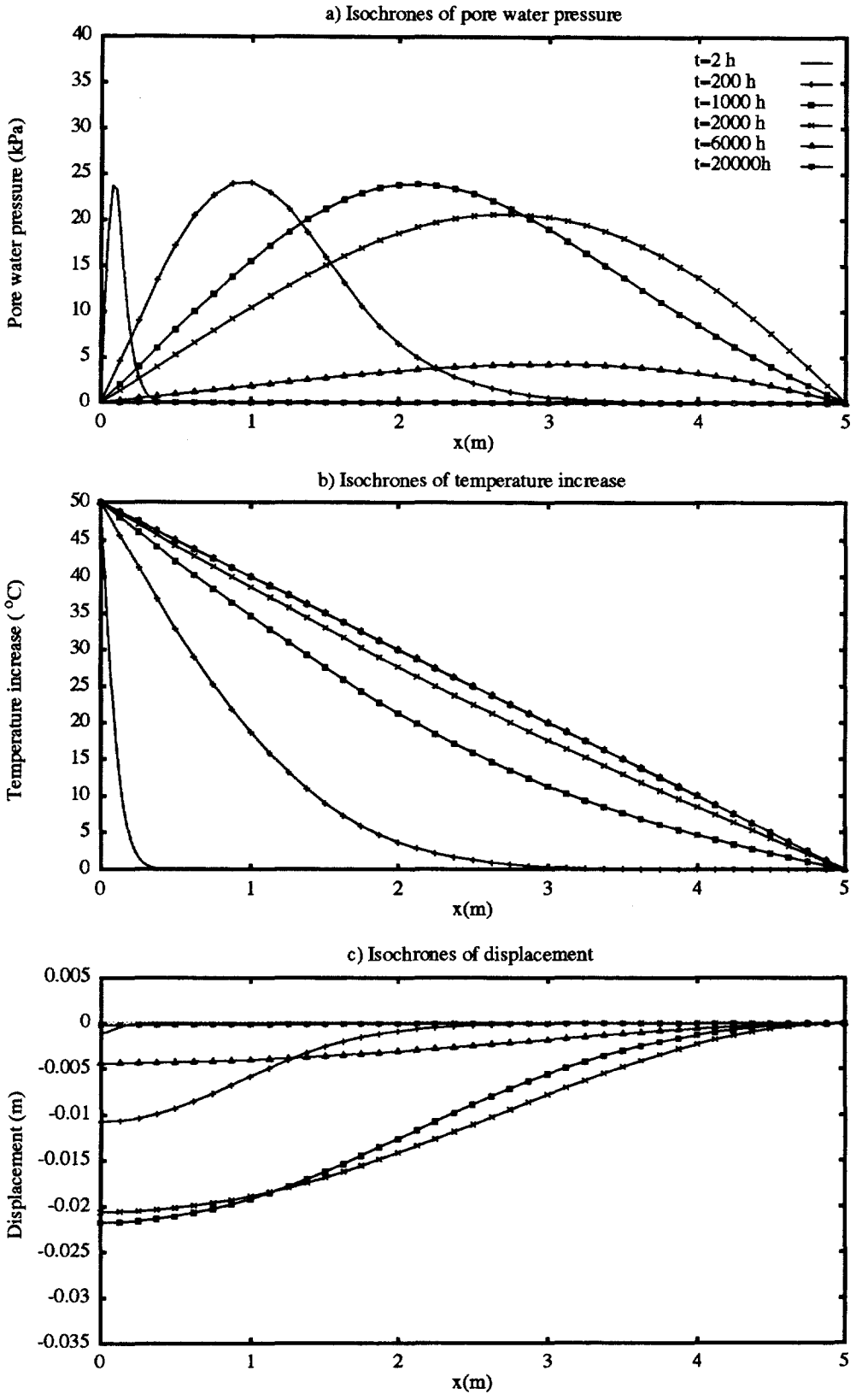

Fig. 4. Finite element solutions of a heated soil column with material property changes (material B).

Figure 5 shows the thermodynamically uncoupled ($S_w = 0$) linear response obtained from eqn (35)–(37) for the same problem. The uncoupled linear model significantly underestimates pore water pressures and displacements. As we have shown before, the temperature distribution is largely independent of the assumptions used in the analysis. The results shown in Figs 1–5 confirm the significance of the thermo-osmosis in thermoporoelastic analysis. The influence of the thermal-filtration appears to be relatively less and possibly negligible. However, further work is needed to study the effect under a wider range of boundary and initial conditions in which these effects may significantly influence the response. It should also be noted that in all example problems the phenomenological coefficient S_w is assumed to be constant due to the availability of limited experimental data. This may not be true for semi-impermeable clay barriers and the consideration of its variations may significantly influence the coupled response.

The final set of results corresponds to the non-linear response of a thick-wall soil cylinder under plane-strain conditions. The inner radius of the cylinder is 0.5 m and the outer radius is 10.5 m. Both surfaces are freely drained. The outer surface is fixed and does not experience a change in temperature. The inner radius is stress free and the temperature is increased by 50°C. This condition idealizes a container of nuclear fuel waste embedded in an extensive thick clay deposit with the properties of material B. Figure 6 shows the pore water pressure, temperature and radial displacement of the cylinder. A moving pore water pressure front is noted with a constant pore water pressure region at early times ($t = 2$ h, and 200 h). The constant pore water pressure region vanishes with increasing time. The peak pore water pressure is developed inside the cylinder nearly 2000 h after the start of heating. The temperature distribution is qualitatively similar to that in a soil column shown earlier except that the steady-state distribution is a logarithmic function of the radius. The displacement isochrones are relatively complicated. The displacement remains inward near the inner wall of the soil cylinder but primarily outward over a larger region. The peak displacement is not observed at the inner surface but inside the cylinder. The inward radial displacement increases with time initially at the inner wall and then decreases. This is a result of the initial expansion of the soil skeleton and water due to heating which causes an increase in pore water pressure. Consequently water drains out causing a reduction in the expansion.

Figure 7 shows the non-linear response of an identical soil cylinder with a constant water pressure of 20 kPa applied to the inner surface in addition to the heating. The boundary conditions at the outer surface are unchanged. The temperature isochrones are almost identical to that in Fig. 6. This implies that the applied pore water pressure gradient has a negligible influence on temperature profiles. However the magnitude of pore water pressure and radial displacement are substantially different from the previous case. A region of constant pore water pressure is noted as in the case of Fig. 6 and the maximum pore water pressure is generated inside the cylinder. Steady-state pore water pressure is reached after 50,000 h. Steady-state pore water pressure distribution is not logarithmic due to the presence thermodynamic coupling. The displacement isochrones are similar to those in Fig. 6 but the magnitude is large. The steady-state displacement is substantially larger than the previous case due to the applied pore water pressure. It takes nearly 6000 h since the heating to reach the maximum displacement of the cylinder. Maximum values of displacement and pore water pressure are not observed at the same point nor do they occur at the same time instants. The numerical results presented in Figs 1–7 confirm the complex coupling effects in a saturated medium under hydro-thermo-mechanical loading. Additional parametric studies on coupled fields are presented elsewhere (Zhou, 1998).

CONCLUSIONS

A coupled thermoporoelastic model accounting for thermodynamically coupled heat–water flow, compressibility and thermal expansion of constituents, changing material properties and convective heat flow is presented. The governing equations of the model are non-linear. It can be reduced to some linear models reported in literature. An explicit analytical solution can be derived for the linear response of a one-dimensional soil column

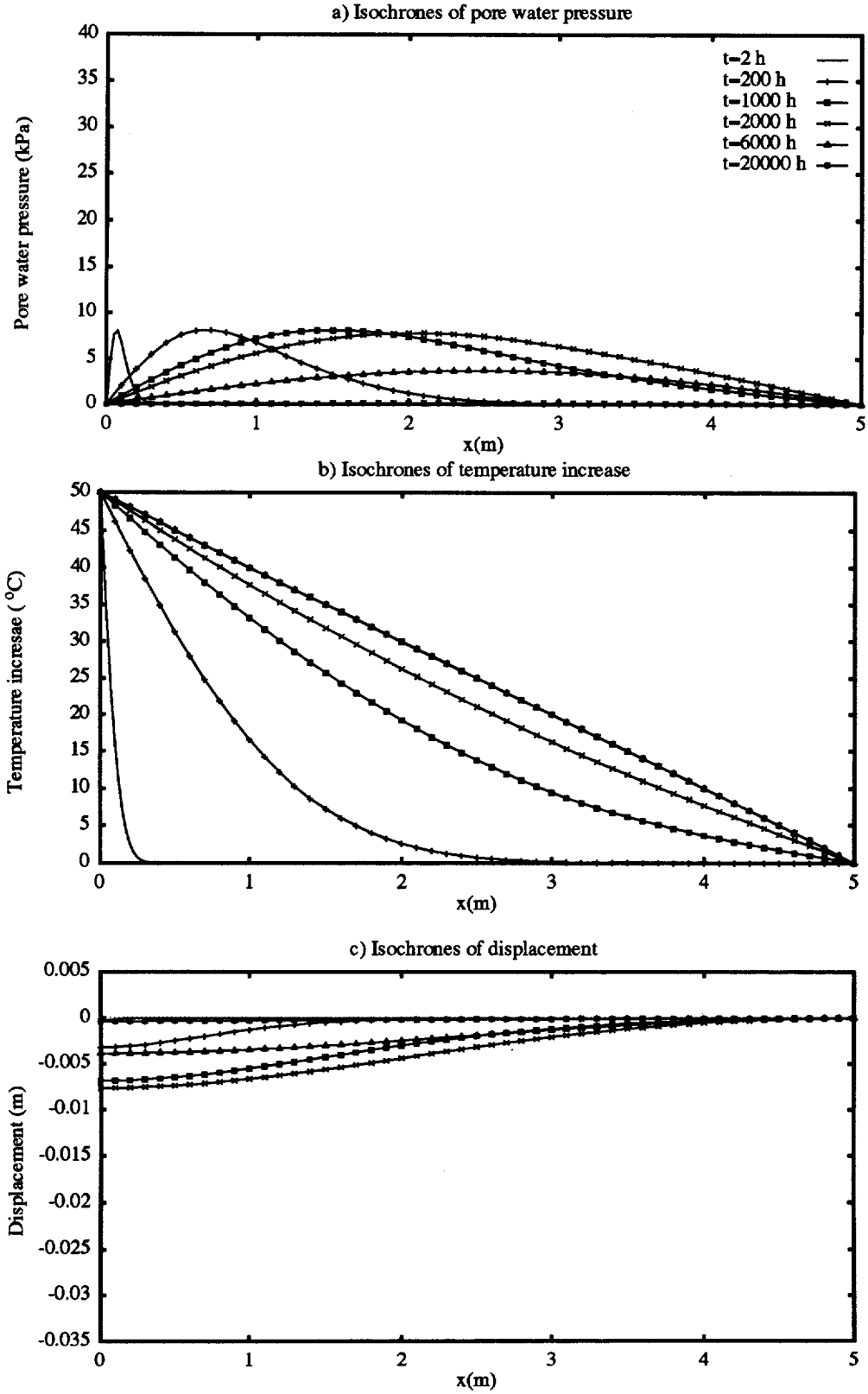

Fig. 5. Semi-coupled analytical solution ($S_w = 0$) of a heated soil column with constant properties (material B).

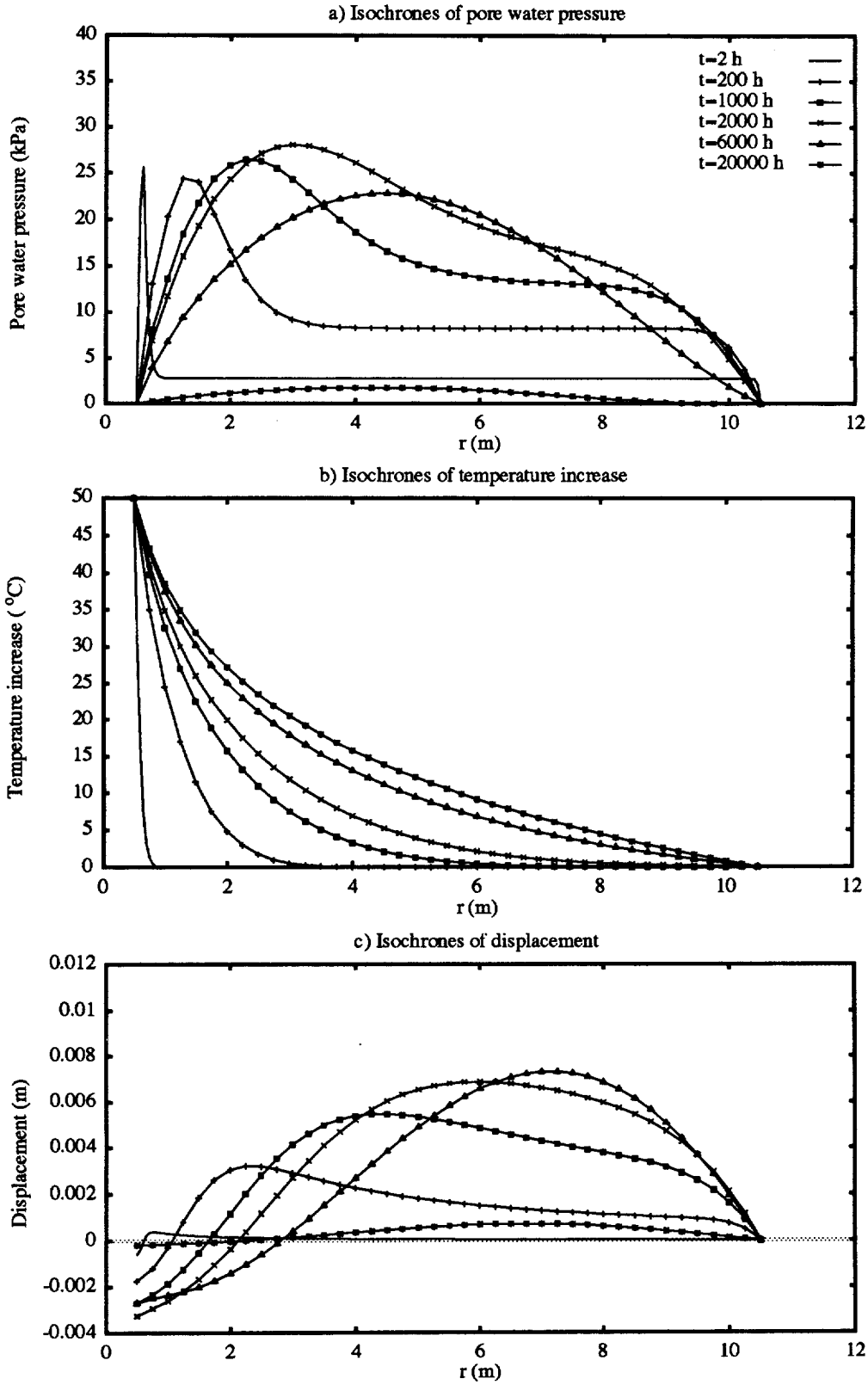

Fig. 6. Finite element solutions of a heated soil cylinder with material property changes (material B).

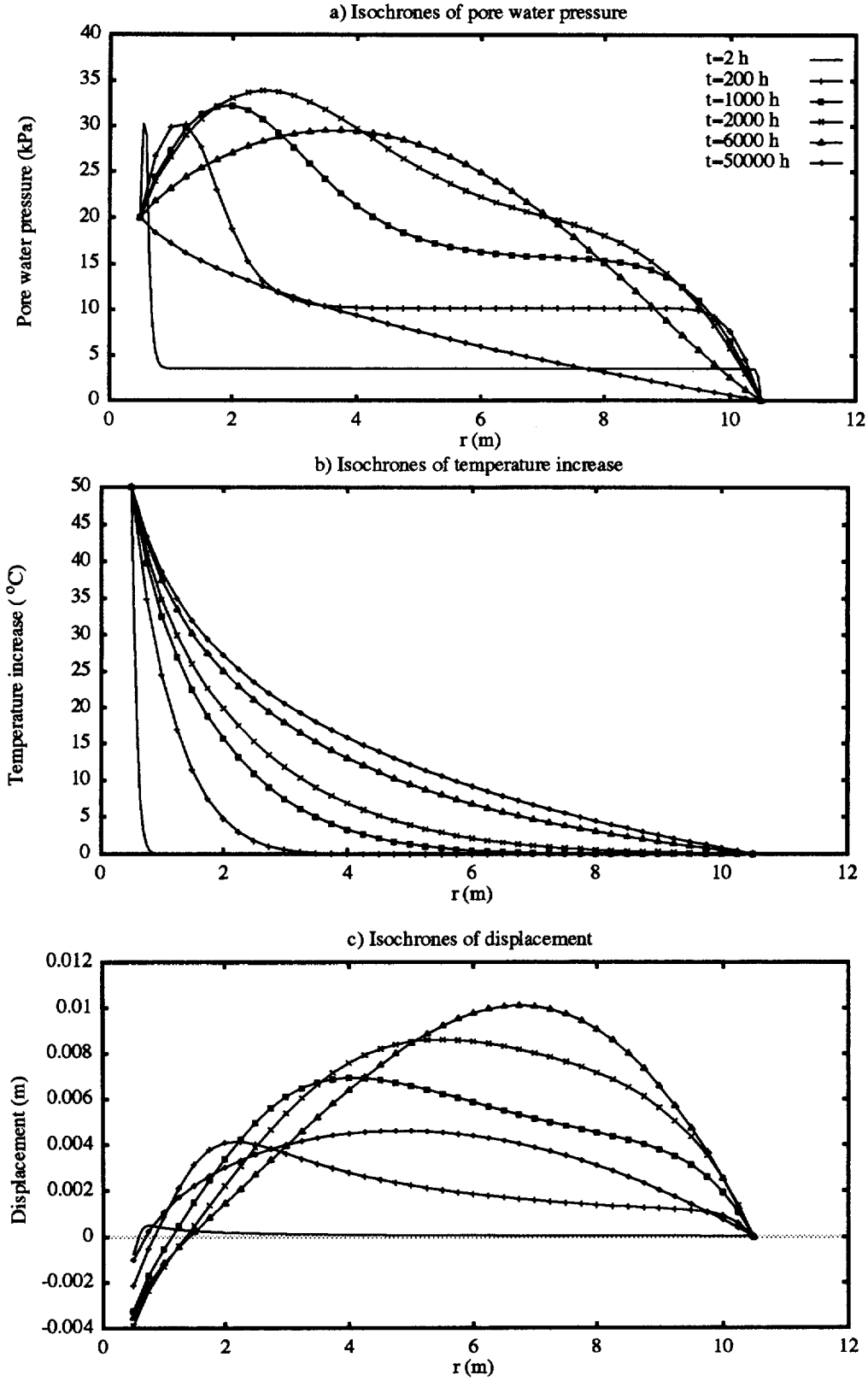

Fig. 7. Finite element solutions of a heated and pressurized soil cylinder with material property changes (material B).

subjected to heating and pressure at one end. The mixed finite element formulation of the non-linear model results in stable solutions over a longer time span. Numerical solutions indicate that the temperature distribution is insignificantly changed due to the presence of thermodynamically coupled heat–water flow and porosity dependent material properties. Substantial differences in pore water pressure and displacements are noted between thermodynamically coupled and uncoupled models. The response predicted by the non-linear model also differs significantly from the linear model. Coupled non-linear fields in cylindrical domain indicate that the inner region of the cylinder experiences the largest displacements and pore water pressures. A complementary experimental program to determine the constitutive properties involved in the present model is essential for realistic modelling of practical problems. The development of a related continuum model for unsaturated media will be reported in the future (Zhou, 1998).

Acknowledgements—The work presented in this paper was supported by the Natural Science and Engineering Research Council of Canada and Atomic Energy Canada Ltd.

REFERENCES

Abramowitz, M. and Stegun, A. (1965) *Handbook of Mathematical Functions*. Dover Publications, New York.
Adkins, J. E. (1963) Non-linear diffusion. I. Diffusion and flow of mixtures of fluids. *Phil. Trans. R. Soc. A* **255,** 607–633.
Bear, J. and Corapcioglu, M. Y. (1981) A mathematical model for consolidation in a thermoelastic quifer due to hot water injection of pumping. *Water Resour. Res.* **17,** 723–736.
Biot, M. A. (1941) General theory of three-dimensional consolidation. *Journal of Applied Physics* **12,** 155–164.
Biot, M. A. (1956) General solutions of the equations of elasticity and consolidation for a porous material. *Journal of Applied Mechanics* **23,** 91–96.
Biot, M. A. (1956) Thermoelasticity and irreversible thermodynamics. *Journal of Applied Physics* **27,** 240–253.
Biot, M. A. (1977) Variational Lagrangian-thermodynamics of nonisothermal finite strain mechanics of porous solids and thermomolecular diffusion. *International Journal of Solids and Structures* **13,** 579–597.
Booker, J. R. and Savvidou, C. (1985) Consolidation around a point heat source. *Int. J. Numer. Anal. Method Geomech.* **9,** 173–184.
Bowen, R. M. (1982) Compressible porous media models by use of the theory of mixtures. *International Journal of Engineering Science* **20,** 697–735.
Britto, A. M., Savvidou, C., Gunn, M. J. and Booker, J. R. (1992) Finite element analysis of the coupled heat flow and consolidation around hot buried objects. *Soils and Foundations* **32,** 13–25.
Carman, P. C. (1937) Fluid flow through a granular bed. *Trans. Inst. Chem. Eng.* **15,** 150–156.
Carnahan, C. L. (1984) Thermodynamic coupling of heat and matter flows in near-field regions of nuclear waste repositories. In *Scientific Basis for Nuclear Waste Management VII*, V26, ed. G. L. McVay, pp. 1023–1030. Elsevier Science Pub. Co., North-Holland, New York.
Chapman, A. J. (1967) *Heat Transfer*. Macmillan, New York.
Coussy, O. (1995) *Mechanics of Porous Continua*. Wiley, New York.
Derski, W. and Kowalski, S. J. (1979) Equations of linear thermoconsolidation. *Arch. Mech.* **31,** 303–316.
Detournay, E. and Cheng, A. H.-D. (1993) Fundamentals of poroelasticity. In *Comprehensive Rock Engineering: Principles, Practice and Projects*, ed. C. Fairhurst, Vol. 2, Chap. 5. Pergamon Press, Oxford.
Farouki, O. T. (1986) *Thermal Properties of Soils*. Trans Tech, Clausthal-Zellerfeld.
Fernandez, R. T. (1972) Natural convection from cylinders buried in porous media. Ph.D. thesis. University of California, Berkeley.
Fitts, D. D. (1962) *Nonequilibrium Thermodynamics: A Phenomenological Theory of Irreversible Processes in Fluid Systems*. McGraw-Hill, New York.
Graham, J., Chandler, N. A., Dixon, D. A., Roach P. J., To, T. and Wan, A. W. L. (1996) The buffer/container experiment: Volume 4—Results, synthesis, issues. Fuel Waste Technology, AECL, Whiteshell Laboratories, Pinawa.
Groenevelt, P. H. and Bolt, G. H. (1969) Non-equilibrium thermodynamics of the soil-water system. *J. Hydrol.* **7,** 358–388.
Hueckel, T. and Pellegrini, R. (1992) Effective stress and water pressure in saturated clays during heating–cooling cycles. *Canadian Geotechnical Journal* **29,** 1095–1120.
Jiang, Q. and Rajapakse, R. K. N. D. (1994) On coupled heat–moisture transfer in deformable porous media. *Q. Jl. Mech. Appl. Math.* **47,** 53–68.
Jumikis, A. R. (1966) *Thermal Soil Mechanics*. Rutgers University Press, New Brunswick, N.J.
Kurashige, M. (1989) A thermoelastic theory of fluid-filled porous materials. *International Journal of Solids and Structures* **25,** 1039–1052.
Letey, J. and Kemper, W. D. (1969) Movement of water and salt through a clay–water system: experimental verification of Onsager's reciprocal relation. *Soil Sci. Soc. Am. Proc.* **33,** 25–29.
Lewis, R. W. and Schrefler, B. A. (1987) *The Finite Element Method in the Deformation and Consolidation of Porous Media*. Wiley, New York.
Lubliner, J. (1990) *Plasticity Theory*. Macmillan, New York.
McNamee, J. and Gibson, R. E. (1960) Displacement functions and linear transforms applied to diffusion through porous elastic media. *Q. Jl. Mech. Appl. Math.* **13,** 98–111.
McTigue, D. (1986) Thermoelastic response of fluid-saturated porous rock. *J. Geophys. Res.* **91,** 9533–9542.

McTigue, D. (1990) Flow to a heated borehole in porous, thermoelastic rock: analysis. *Water Resour. Res.* **26,** 1763–1774.
McVay, G. L. (1984) *Scientific Basis for Nuclear Waste Management VII*, V26. Elsevier Science Pub. Co., North-Holland, New York.
Noorishad, J., Tsang, C. F. and Witherspoon, P. A. (1984) Coupled thermal–hydraulic–mechanical phenomena in saturated fractured porous rocks: numerical approach. *J. Geophys. Res.* **89,** 10,365–10,373.
Onsager, L. (1931) Reciprocal relations in irreversible processes. I. *Physical Review* **37,** 403–426.
Palciauskas, V. V. and Domenico, P. A. (1982) Characterization of drained and undrained response of thermally loaded repository rocks. *Water Resour. Res.* **18,** 281–290.
Rice, J. R. and Cleary, M. P. (1976) Some basic stress–diffusion solutions for fluid saturated elastic porous media with compressible constituents. *Rev. Geophys. Space Phys.* **14,** 227–241.
Schiffman, R. L. (1971) A thermoelastic theory of consolidation. In *Environmental and Geophysical Heat Transfer*, pp. 78–84. ASME, New York.
Seneviratne, H. N., Carter, J. P. and Booker, J. R. (1994) Analysis of fully coupled thermomechanical behaviour around a rigid cylindrical heat source buried in clay. *Int. J. Numer. Anal. Method Geomech.* **18,** 177–203.
Senjuntichai, T. (1994) Green's functions for multi-layered poroelastic media and an indirect boundary element method. Ph.D. thesis, University of Manitoba, Winnipeg.
Smith, D. and Booker, J. (1993) Green's functions for a fully coupled thermoporoelastic material. *Int. J. Numer. Anal. Methods Geomech.* **17,** 139–163.
Srivastava, R. C. and Avasthi, P. K. (1975) Non-equilibrium thermodynamics of thermo-osmosis of water through kaolinite. *J. Hydrol.* **24,** 111–120.
Tanaka, N. and Graham, J. (1996) Pore water pressures in undrained triaxial tests with heating. *The 2nd International Congress on Environmental Geotechnics*, Osaka, Japan.
Zhou, Y. (1998) Non-linear thermo–hydro–mechanical behavior of saturated and unsaturated porous media. Ph.D. thesis, University of Manitoba.
Zienkiewicz, O. C. (1977) *The Finite Element Method.* McGraw-Hill, New York.

APPENDIX A

Applying Laplace transforms to eqns (30)–(32) results in,

$$\frac{1-\nu}{1-2\nu}2G\frac{\partial^2}{\partial x^2}\bar{\varepsilon}_v-\xi\frac{\partial^2}{\partial x^2}\bar{p}-K'\alpha\frac{\partial^2}{\partial x^2}\bar{T}=0 \tag{A1}$$

$$k\frac{\partial^2}{\partial x^2}\bar{p}+S_w\frac{\partial^2}{\partial x^2}\bar{T}=c_1s\bar{\varepsilon}_v-c_2s\bar{T}+c_3s\bar{p} \tag{A2}$$

$$C_vs\bar{T}-T_0K'\alpha s\bar{\varepsilon}_v=(\lambda-T_0\alpha_w\beta_wS_w)\frac{\partial^2}{\partial x^2}\bar{T}+T_0(S_w-\alpha_w\beta_wk)\frac{\partial^2}{\partial x^2}\bar{p} \tag{A3}$$

where s is the Laplace transform variable, and an overbar ($^-$) is hereafter used to identify the Laplace transform of a variable.

From eqn (A2),

$$\bar{\varepsilon}_v=\frac{S_w}{c_1s}\frac{\partial^2}{\partial x^2}\bar{T}+\frac{k}{c_1s}\frac{\partial^2}{\partial x^2}\bar{p}+\frac{c_2}{c_1}\bar{T}-\frac{c_3}{c_1}\bar{p} \tag{A4}$$

Substitution of eqn (A4) into eqn (A3) results in

$$a_1\frac{\partial^2}{\partial x^2}\bar{T}+a_2\frac{\partial^2}{\partial x^2}\bar{p}+a_3s\bar{T}+a_4s\bar{p}=0 \tag{A5}$$

where

$$a_1=-\frac{T_0K'\alpha S_w}{c_1}-\lambda+T_0\alpha_w\beta_wS_w;\quad a_2=-\frac{T_0K'\alpha k}{c_1}-T_0(S_w-\alpha_w\beta_wk)$$
$$a_3=-\frac{T_0K'\alpha c_2}{c_1}+C_v,\quad a_4=\frac{T_0K'\alpha c_3}{c_1} \tag{A6}$$

Integration of eqn (A1) results in the following general solution

$$\frac{1-\nu}{1-2\nu}2G\bar{\varepsilon}_v-\xi\bar{p}-K'\alpha\bar{T}=d_1x+d_2 \tag{A7}$$

where d_1 and d_2 are unknown constants to be determined by boundary conditions and the equilibrium equation expressed in terms of stresses.

Substitution of eqn (A4) in eqn (A7) yields

$$b_1\frac{\partial^2}{\partial x^2}\bar{T}+b_2\frac{\partial^2}{\partial x^2}\bar{p}+b_3 s\bar{T}+b_4 s\bar{p}=s(d_1x+d_2) \tag{A8}$$

where

$$b_1=\frac{(1-\nu)2GS_w}{(1-2\nu)c_1};\quad b_2=\frac{(1-\nu)2Gk}{(1-2\nu)c_1}$$
$$b_3=\frac{(1-\nu)2Gc_2}{(1-2\nu)c_1}-K'\alpha;\quad b_4=-\frac{(1-\nu)2Gc_3}{(1-2\nu)c_1}-\xi \tag{A9}$$

Elimination of $(\partial^2/\partial x^2)T$ from eqn (A8) by using eqn (A5) results in

$$\bar{T}=\frac{h_1}{s}\frac{\partial^2}{\partial x^2}\bar{p}+h_2\bar{p}+h_3(d_1x+d_2) \tag{A10}$$

where

$$h_1=-\frac{a_1b_2-b_1a_2}{a_1b_3-a_3b_1};\quad h_2=-\frac{a_1b_4-b_1a_4}{a_1b_3-a_3b_1};\quad h_3=\frac{a_1}{(a_1b_3-a_3b_1)} \tag{A11}$$

Substitution of eqn (A10) into eqn (A5) results in,

$$g_1\frac{\partial^4}{\partial x^4}\bar{p}+g_2 s\frac{\partial^2}{\partial x^2}\bar{p}+g_3 s^2\bar{p}+\frac{a_3h_3s^2(d_1x+d_2)}{a_1}=0 \tag{A12}$$

where

$$g_1=h_1;\quad g_2=\frac{a_2}{a_1}+h_2+\frac{a_3}{a_1}h_1;\quad g_3=\frac{a_4}{a_1}+\frac{a_3}{a_1}h_2 \tag{A13}$$

The general solution of eqn (A11) is

$$\bar{p}=A_1\,e^{\gamma_1\sqrt{sx}}+B_1\,e^{-\gamma_1\sqrt{sx}}+A_2\,e^{\gamma_2\sqrt{sx}}+B_2\,e^{-\gamma_2\sqrt{sx}}+h_0(d_1x+d_2) \tag{A14}$$

where

$$\gamma_1^2=\frac{-g_2-\sqrt{g_2^2-4g_1g_3}}{2g_1};\quad \gamma_2^2=\frac{-g_2+\sqrt{g_2^2-4g_1g_3}}{2g_1};\quad h_0=-\frac{a_3h_3}{a_1g_3} \tag{A15}$$

Substitution of eqn (A14) into eqn (A10) results in,

$$\bar{T}=(h_1\gamma_1^2+h_2)(A_1\,e^{\gamma_1\sqrt{sx}}+B_1\,e^{-\gamma_1\sqrt{sx}})+(h_1\gamma_2^2+h_2)(A_2\,e^{\gamma_2\sqrt{sx}}+B_2\,e^{-\gamma_2\sqrt{sx}})+(h_0h_2+h_3)(d_1x+d_2) \tag{A16}$$

It can be shown from eqn (A4), (A14) and (A16) that

$$\bar{\varepsilon}_v=E_1(A_1\,e^{\gamma_1\sqrt{sx}}+B_1\,e^{-\gamma_1\sqrt{sx}})+E_2(A_2\,e^{\gamma_2\sqrt{sx}}+B_2\,e^{-\gamma_2\sqrt{sx}})+f(d_1x+d_2) \tag{A17}$$

where

$$E_1=[\xi+K'\alpha(h_1\gamma_1^2+h_2)]\Big/\left(\frac{1-\nu}{1-2\nu}2G\right) \tag{A18a}$$

$$E_2=[\xi+K'\alpha(h_1\gamma_2^2+h_2)]\Big/\left(\frac{1-\nu}{1-2\nu}2G\right) \tag{A18b}$$

$$f=[1+\xi h_0+K'\alpha(h_0h_2+h_3)]\Big/\left(\frac{1-\nu}{1-2\nu}2G\right) \tag{A18c}$$

The following solution for axial displacement of the column can be determined by using eqn (A17).

$$\bar{u}_x=\frac{E_1}{\gamma_1\sqrt{s}}(A_1\,e^{\gamma_1\sqrt{sx}}-B_1\,e^{-\gamma_1\sqrt{sx}})+\frac{E_2}{\gamma_2\sqrt{s}}(A_2\,e^{\gamma_2\sqrt{sx}}-B_2\,e^{-\gamma_2\sqrt{sx}})+f(d_1x^2/2+d_2x)+d_3 \tag{A19}$$

where d_3 is an unknown constant to be determined by boundary conditions.

It can be shown by using the equilibrium equation that

$$d_1 = 0 \tag{A20}$$

The remaining six unknowns d_2, d_3, A_1, A_2, B_1 and B_2 can be determined by using the six boundary conditions given by eqn (33). Thereafter, the time-domain solution is obtained by performing inverse Laplace transform analytically.

APPENDIX B

The coefficients ζ_i ($i = 1, \ldots, 6$) in eqn (41) are defined as

$$\zeta_1 = (T+T_0)\left[na_w + \frac{(1-n)\alpha K'}{c_1 K_s}\right]$$

$$\zeta_2 = C_v - (T+T_0)\left\{na_w^2\beta_w - \frac{\alpha[K'\alpha - K_s(1-n)a_s]K'}{c_1 K_s}\right\}$$

$$\zeta_3 = (T+T_0)\left(a_w\beta_w - \frac{\alpha K'}{c_1}\right); \quad \zeta_4 = C_w\left[\rho_w k + \rho_{w0}T\left(-a_w k + \frac{S_w}{\beta_w}\right)\right]$$

$$\zeta_5 = \frac{\rho_{w0}C_w kT}{\beta_w}; \quad \zeta_6 = C_w S_w(\rho_w - a_w\rho_{w0}T) \tag{A21}$$

The matrices **G** and **K** and vectors **X** and **F** in eqn (44) can be expressed as

$$\mathbf{G} = \begin{bmatrix} 0 & 0 & 0 & 0 \\ 0 & \mathbf{G}_{22} & \mathbf{G}_{23} & \mathbf{G}_{24} \\ 0 & \mathbf{G}_{32} & \mathbf{G}_{33} & \mathbf{G}_{34} \\ \mathbf{G}_{41} & \mathbf{G}_{42} & \mathbf{G}_{43} & \mathbf{G}_{44} \end{bmatrix}; \quad \mathbf{K} = \begin{bmatrix} \mathbf{K}_{11} & \mathbf{K}_{12} & \mathbf{K}_{13} & 0 \\ 0 & \mathbf{K}_{22} & \mathbf{K}_{23} & 0 \\ 0 & \mathbf{K}_{32} & \mathbf{K}_{33} & \mathbf{K}_{34} \\ 0 & 0 & 0 & 0 \end{bmatrix}$$

$$\mathbf{X} = \begin{bmatrix} \hat{\mathbf{U}}(t) \\ \hat{\mathbf{P}}(t) \\ \hat{\mathbf{T}}(t) \\ \hat{\mathbf{n}}(t) \end{bmatrix}; \quad \mathbf{F} = \begin{bmatrix} \mathbf{F}_1 \\ \mathbf{F}_2 \\ \mathbf{F}_3 \\ 0 \end{bmatrix} \tag{A22}$$

where

$$\mathbf{G}_{22} = \int_\Omega \mathbf{N}^T \frac{n}{\beta_w}\mathbf{N}\,d\Omega, \quad \mathbf{G}_{23} = -\int_\Omega \mathbf{N}^T na_w\mathbf{N}\,d\Omega, \quad \mathbf{G}_{24} = \int_\Omega \mathbf{N}^T\mathbf{N}\,d\Omega$$

$$\mathbf{G}_{32} = \int_\Omega \mathbf{N}^T\zeta_1\mathbf{N}\,d\Omega, \quad \mathbf{G}_{33} = \int_\Omega \mathbf{N}^T\zeta_2\mathbf{N}\,d\Omega, \quad \mathbf{G}_{34} = \int_\Omega \mathbf{N}^T\zeta_3\mathbf{N}\,d\Omega$$

$$\mathbf{G}_{41} = \int_\Omega \mathbf{N}^T c_1\mathbf{m}\mathbf{B}\,d\Omega, \quad \mathbf{G}_{42} = \int_\Omega \mathbf{N}^T\frac{1-n}{K_s}\mathbf{N}\,d\Omega$$

$$\mathbf{G}_{43} = \int_\Omega \mathbf{N}^T\left[\frac{K'}{K_s}\alpha - (1-n)a_s\right]\mathbf{N}\,d\Omega, \quad \mathbf{G}_{44} = -\int_\Omega \mathbf{N}^T\mathbf{N}\,d\Omega$$

$$\mathbf{K}_{11} = \int_\Omega \mathbf{B}^T\mathbf{D}\mathbf{B}\,d\Omega, \quad \mathbf{K}_{12} = -\int_\Omega \xi\mathbf{B}^T\mathbf{m}^T\mathbf{N}\,d\Omega, \quad \mathbf{K}_{13} = -\int_\Omega \mathbf{B}^T K'\alpha\mathbf{m}^T\mathbf{N}\,d\Omega$$

$$\mathbf{K}_{22} = \int_\Omega \nabla\mathbf{N}^T k\nabla\mathbf{N}\,d\Omega, \quad \mathbf{K}_{23} = \int_\Omega \nabla\mathbf{N}^T S_w\nabla\mathbf{N}\,d\Omega$$

$$\mathbf{K}_{32} = -\int_\Omega \mathbf{N}^T\left(\frac{1}{2}\zeta_4\nabla T + \zeta_5\nabla p\right)\nabla\mathbf{N}\,d\Omega + \int_\Omega \nabla\mathbf{N}^T S_w^*\nabla\mathbf{N}\,d\Omega$$

$$\mathbf{K}_{33} = \int_\Omega \nabla\mathbf{N}^T\frac{1}{2}[2\lambda_s + (\lambda_w - \lambda_s)n]\nabla\mathbf{N}\,d\Omega - \int_\Omega \mathbf{N}^T\left(\frac{1}{2}\zeta_4\nabla p + \zeta_6\nabla T\right)\nabla\mathbf{N}\,d\Omega$$

$$\mathbf{K}_{34} = \int_\Omega \nabla\mathbf{N}^T\frac{1}{2}(\lambda_w - \lambda_s)\nabla T\mathbf{N}\,d\Omega$$

$$\mathbf{F}_1 = \int_S \mathbf{N}^T\mathbf{t}\,dS, \quad \mathbf{F}_2 = \int_S \mathbf{N}^T\mathbf{q}_{\text{liq}}\cdot d\mathbf{S}, \quad \mathbf{F}_3 = \int_S \mathbf{N}^T\mathbf{q}_T\cdot d\mathbf{S} \tag{A23}$$

and $\mathbf{q}_{\text{liq}}$ and $\mathbf{q}_T$ denote the specified water and heat (conductive) fluxes at the boundary **S**.